

An alternative methodology to assess the quality of empirical potentials for small gold clusters

Luis A. Mancera^{a,*}, David M. Benoit^b

^a*Institute of Theoretical Chemistry, University of Ulm, Albert-Einstein-Allee 11, D-89069 Ulm, Germany*

^b*The University of Hull, Cottingham Road, Kingston upon Hull HU6 7RX, U.K.*

Abstract

We present a methodology based on local comparisons of potential energy surfaces (PES) in order to assess the quality of empirical potentials. We compare five typical empirical potentials using a criterion that shows which of these potentials resembles better a PES obtained with a high-level electronic structure method. The methodology relies on a many-body expansion in terms of normal coordinates of both the empirical and high-level theory PES. Then we investigate in a systematic way, how the features of the reference high-level theory PES are reproduced by each empirical potential in the vicinity of a given minimum energy structure. We use plane-wave density functional theory (DFT) as a reference, in particular the Perdew-Burke-Ernzerhof (PBE) exchange-correlation functional and an ultrasoft Vanderbilt pseudo potential. This study is carried out on neutral gold clusters with up to five atoms.

Keywords: empirical potentials, gold clusters, potential energy surfaces

PACS: 34.20.Cf, 61.46.Bc, 31.50.BC

1. Introduction

Two-body potentials are widely used to study noble gases but show several limitations in describing metallic systems accurately. [1] To overcome such limitations, some empirical potentials including many-body effects have been developed. Most comparative studies of empirical potentials focus on analyzing how the minimum energy structures are reproduced in comparison with high-level theory methods. The most frequent comparisons include binding energies, bond lengths and sometimes harmonic frequencies. Although this type of analysis provides an approximate description of the behavior of these potentials, it is often not sufficient for knowing their relative advantages or estimating which of them better resembles high-level theory results.

The first drawback of a simple and direct comparison between empirical potentials is that they have different analytical expressions. For example, the Murrell-Mottram potential [2, 3] contains two- and three-body terms, while others contain both a repulsive pair term and a cohesive many-body term, such as the Gupta [4, 5] and the Sutton-Chen [6] potentials. Some models contain a pair-interaction term and a many-body term with a non-linear function based on the features of the atomic environment. The Voter-Chen [7–9] and the Daw-Baskes-Foiles (DBF) [10, 11] versions of the embedded atom model (EAM), and the Glue potential [1] are some of such models. The function of the many-body term of the Glue model associates an energy value to the coordination of each atom. The function of

the many-body term of the EAM expresses the energy in terms of the background electron density and the atomic species. The Voter-Chen and the DBF potentials have different forms for the pair-interaction and the many-body parts; *e.g.* the Voter-Chen potential uses a Morse-type term for the pair interaction, while in the DBF potential such an interaction is entirely repulsive. An additional drawback of a direct comparison is the fact that the empirical parameters are often fitted to different experimental values, and they do not always correspond to the same quantities. Therefore, we introduce here a local comparison of potential energy surfaces (PES) around a given minimum energy structure as an alternative way to assess the quality of empirical potentials. We use normal coordinates, which are defined in terms of the mass-weighted cartesian displacement coordinates, since these offer a practical way to explore the surface landscape around the minimum.

We carry out our investigation on small neutral gold clusters. This type of clusters are often used as probe systems for testing theoretical methods, due mainly to relativistic effects, [12–15] that give them some peculiar properties. In addition, they are of great technological interest due to possible applications in several fields, such as catalysis, sensors, molecular electronics, and gene mapping. [14–16] Empirical potentials are often cataloged as unreliable for describing structural and energetic properties accurately compared to high-level theory, for example for reproducing the planar structures of small gold clusters. In addition, in the regime of very small sizes direct optimization at the DFT or higher level is possible, although studies are often focused on interesting particular sizes. This is the case of the systematic studies carried out on the Au₈ cluster by Serapian *et al.* [17] or on Au_{8–n}Au_n bimetallic clusters by Heiles *et al.*, [18] in order to understand the transition from 2D to 3D structures. In spite of

*Corresponding author

Email addresses: luis.mancera@uni-ulm.de (Luis A. Mancera), d.benoit@hull.ac.uk (David M. Benoit)

that, our methodology is useful in order to choose comparatively reliable empirical potentials to be used in those cases in which the use of DFT or higher level electronic structure methods is still limited or prohibitive. It is also applicable to clusters of another atom species different than gold.

Several studies have been carried out on gold clusters using empirical potentials, [19–29] but only a few of them have performed a comparison of different potentials. Wilson and Johnston [19] compare global minimum energy structures obtained with the Murrell-Mottram potential with those obtained from the Gupta and the Sutton-Chen potentials. They found that the minimum energy structures obtained for all of these potentials are similar up to Au₇ only. Rogan *et al.* [30] compare the results of the Murrell-Mottram and the DBF potentials with DFT calculations for gold clusters up to $n = 12$. They found that the DBF potential largely overestimates the binding energies compared to the Perdew-Burke-Ernzerhof (PBE) functional [31] using a norm-conserving pseudo potential. Grigoryan *et al.* [28] use a relation of similarity to evaluate the differences at all interatomic distances between two structures with equivalent geometries. They found that the Voter-Chen and DBF potentials work similarly for Cu and Ni, but they show large differences for Au clusters with $n < 20$. Hermann *et al.* [32] compare empirical potentials to second-order Møller-Plesset perturbation theory (MP2) calculations, using a many-body decomposition of the interaction potential. Their study focuses on the Au₇ cluster, which was found to be non-planar at the MP2 level of theory, and shows that the many-body terms converge very slowly for MP2 and very rapidly for the empirical potentials.

The remainder of this paper is organized as follows: In Section 2, we describe the methodology and relevant computational details of our investigation. In Section 3, we describe the criteria used to choose a suitable DFT approach as a reference. In Section 4 we present the assessment of the empirical potentials, and in Section 5 we give our conclusions.

2. Methodology and computational details

Our analysis is carried out in two steps: First, we compare structural parameters and binding energies obtained using the empirical potentials with those obtained using a chosen DFT approach, for cluster sizes up to $N = 10$. This is a usual standard comparison but contrary to previous studies, we also consider structures with geometries equivalent to the global DFT minimum structures. We must impose some constraints to the empirical potentials in order to obtain planar gold clusters as DFT does. Second, we carry out a local comparison of the PES around the minimum energy structure obtained using both an empirical potential and DFT, for each cluster size up to $N = 5$. In this case, we explore the PES using a hierarchical many-body expansion in terms of a set of n mass-weighted normal coordinates, limited to the second order in V (pairwise approximation): [33, 34]

$$V(\mathbf{Q}) = E_0 + \sum_i^n V_i^{(1)}(Q_i) + \sum_i^n \sum_{i < j}^n V_{i,j}^{(2)}(Q_i, Q_j). \quad (1)$$

The number of mass-weighted normal coordinates in $\mathbf{Q} = \{Q_1, \dots, Q_n\}$ corresponds to the number of vibrational modes and is determined by the number of atoms N , *i.e.* $n = 3N - 6$ for non-linear structures or $n = 3N - 5$ for linear structures such as Au₂. The potential $V(\mathbf{Q})$ is explored only locally with $V_i^{(1)}(Q_i)$ corresponding to the single-mode contributions (diagonal or 1D) and $V_{i,j}^{(2)}(Q_i, Q_j)$ corresponding to the pairwise contributions (coupled or 2D). 1D contributions to the PES describe how the potential changes when the normal coordinates change in one direction. 2D contributions describe how the potential changes due to the coupling of displacements in two different directions. These contributions are expressed as:

$$V_i^{(1)}(Q_i) = V(Q_i) - E_0, \quad (2)$$

$$V_{i,j}^{(2)}(Q_i, Q_j) = V(Q_i, Q_j) - V_i^{(1)}(Q_i) - V_j^{(1)}(Q_j) - E_0, \quad (3)$$

For the comparison of the 1D contributions to the PES, we compute first the deviation from the harmonic potential as:

$$\tilde{V}_i^{(1)}(Q_i) = V_i^{(1)}(Q_i) - V_i^{(harm)}(Q_i), \quad (4)$$

where the harmonic potential is computed directly from the 1D curves as:

$$V_i^{(harm)}(Q_i) = \frac{1}{2} \left(\frac{\partial^2 E}{\partial Q_i^2} \right)_0 Q_i^2. \quad (5)$$

We define a 1D index, in terms of the potential evaluated on a number (n^{max}) of grid points. This is done in order to assign a magnitude to the global variations of the 1D contributions in each direction,

$$\zeta_i^{1D} = \frac{1}{n^{max}} \sum_{n_i}^{n^{max}} |\tilde{V}_i^{(1)}(n_i)|. \quad (6)$$

Correspondingly, in order to assign a magnitude to the global variations of the 2D PES, we define a 2D index,

$$\zeta_{ij}^{2D} = \frac{1}{(n^{max})^2} \sum_{n_i}^{n^{max}} \sum_{n_j}^{n^{max}} |V_{ij}^{(2)}(n_i, n_j)|. \quad (7)$$

Both indices, ζ_i^{1D} and ζ_{ij}^{2D} , of each normal coordinate or pair-coupled normal coordinates, are useful quantities for comparing the PES predicted by each empirical potential and by the chosen high-level theory.

To obtain the DFT total energies we perform plane-wave DFT calculations using version 3.11.1 of the CPMD code. [35] The

choice of a DFT exchange-correlation functional to be used as a reference for the comparison was based on the study of four different functionals applied to the gold clusters. We tested the PBE, [31] BP86, [36, 37] BLYP [36, 38] and LDA [39] functionals with Vanderbilt (VDB) pseudo potentials. [40] The Vanderbilt approach is an alternative model to the norm-conserving pseudo potentials (NCPP). Studies have shown that the NCPP work well within LDA using plane-wave basis functions, but are problematic for systems containing highly localized valence orbitals such as transition metals. [40] Vanderbilt pseudo potentials, also known as ultrasoft pseudo potentials (USPP), are norm-conserving in a general sense with an accuracy exceeding that of NCPP. Low cutoffs between 20-30 Ry are required, while other pseudo potentials require larger cutoffs (above 100 Ry). The pseudo potentials used in this study have been generated using a relativistic wave equation for the all-electron case. However, spin-orbit effects are not included. To our knowledge, ultrasoft pseudo potentials have only been used in the study of small gold clusters by Majunder *et al.* [41] and by Olson *et al.* [42]

We use a Vanderbilt pseudo potential basis set, [40] which includes the $5d^{10}6s^1$ gold valence electrons with a plane-wave energy cutoff of 30 Ry (408 eV). We use periodic boundary conditions and a cubic supercell of $(15 \text{ \AA})^3$ to avoid interactions between neighboring clusters. The convergence criteria for wave function and geometry optimizations are set to 10^{-7} a.u. (largest element of the gradient for the wave function) and 5×10^{-5} a.u. (largest element of the gradient for the ions), respectively. We set parameter DUAL to 6.0 (ratio between the wave function energy cutoff and the density cutoff) and GC-CUTOFF to 10^{-5} (density cutoff for calculation of the gradient correction), in order to guarantee a smooth convergence of the wave function optimization. Geometry optimization is carried out by means of the limited-memory BFGS (L-BFGS) [43] method, starting from structures obtained with the Gupta potential. Hessian matrix is calculated using the finite differences of analytical first derivatives with a step length of 10^{-2} bohr. The local spin density approximation (LSD) version of the functional is used for clusters with an odd number of atoms. The few MP2 calculations in this study are performed using the GAMESS-US code [44] and the SBKJJC(1f) basis set, which corresponds to the standard SBKJJC basis set [45] and effective scalar relativistic core potential (ECP) with an extra set of functions f (exponent=0.89). [46]

To obtain the total energies for each empirical potential, we use the Nelder and Mead version of the Simplex method [47–49] in order to minimize a set of random initial geometries for each cluster size. We use version 1.0 of the EPOCUS code, [50] an own program written for this purpose. In each case, a total of 1000 initial geometries are sampled and converged to local minimum energy structures. The Nelder and Mead method converges quickly since it does not require the calculation of derivatives. It also only needs one or two evaluations of the potential function at each step (only in a few cases it requires $m + 1$ or $m + 2$ evaluations, where m is the number of vertices of the simplex). By exploring an extensive set of initial structures, we found that the lowest local minima obtained coincide with the global minimum energy structures reported using other types of global minimization methods. To reproduce planar structures similar

to those predicted by DFT and *ab initio* methods, constraints are employed in the minimization.

The PES construction is performed using the PVSCF code [51] which drives either the CPMD [35] code or the EPOCUS [50] code, in order to calculate the total energy of different geometries that are defined by the variation of the normal coordinates around the global minimum structures. Starting from an optimised structure and its corresponding Hessian matrix, we evaluate the DFT total energy or total empirical energy for a fixed number of points on a grid (here 16) to obtain the 1D potential energies, and for a regular grid with 256 points (16×16) to obtain the 2D PES. The 16 regularly spaced grid points along each normal coordinate are interpolated to a finer-meshed representation of the PES using a cubic-spline algorithm. The 256 regularly spaced grid points for each mode–mode coupling term are interpolated on a finer mesh using a bicubic interpolation. [52]

Cluster binding energies are calculated as the difference between the total energy of the cluster and the sum of the energies of the isolated gold atoms. They are reported positive as a convention. Clusters are visualized using the Visual Molecular Dynamics (VMD) program. [53]

3. Choice of a reference DFT approach

Before assessing the empirical potentials we apply the methodology introduced in Section 2 in order to compare various DFT approaches and find one of them to be used as the reference. Although DFT has limitations to properly account for dispersion contributions to the energy, this is supposed to be not critical in this study, since for these cluster sizes intracuster van der Waals (vdW) contribution are small, as it has been reported by Ghiringhelli *et al.* [54] who use PBE+vdW and numeric atom-centered basis functions in order to include dispersion contributions. They reported zero intracuster van der Waals (vdW) contribution for Au_2 and Au_3 , and -5 meV/atom for Au_4 . We compute the 1D potential energy curve for Au_2 as well as the 1D and 2D potential energies for Au_3 , around the minimum energy structure obtained from different DFT functionals. The number of 1D indices correspond to the number of normal coordinates, n . For Au_2 , there is only one 1D index (ζ_1^{1D}), which corresponds to the unique normal coordinate. For Au_3 , there are three 1D indices (ζ_1^{1D} , ζ_2^{1D} and ζ_3^{1D}). The number of 2D indices is determined by the n normal coordinates, as $n(n-1)/2$. For Au_3 , there are three 2D indices ($\zeta_{1,2}^{2D}$, $\zeta_{1,3}^{2D}$ and $\zeta_{2,3}^{2D}$).

Figure 1 shows the 1D potential energy curves of Au_2 for the various DFT approaches studied. Only the one for LDA differs significantly from the others. Table 1 shows all calculated indices. For Au_2 and Au_3 , LDA leads to the largest values of the 1D index. For Au_3 with all functionals, the larger differences correspond to ζ_2^{1D} , which describes the breathing mode of the molecule. The values of the 2D indices for Au_3 are very similar using PBE and BP86. For LDA and BLYP the differences in 2D energies, given by the value of the index, are significantly larger when compared to PBE or BP86. In the case of LDA, such differences are positive, showing the usual overbinding due to this functional. The larger 2D index for Au_3 corresponds to

$\zeta_{1,2}^{2D}$ which accounts for the coupling between the stretching and the breathing mode of the molecule.

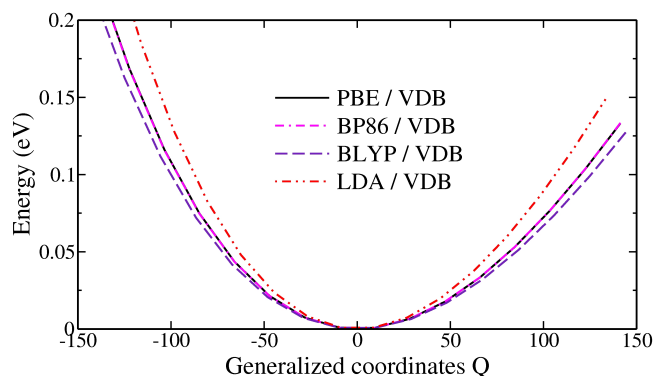


Figure 1: 1D potential energy curves for Au₂, using various DFT approaches.

Table 1: Comparison of various DFT approaches using a Vanderbilt pseudo potential. 1D indices for Au₂ and Au₃, and 2D indices for Au₃, scaled by 10³.

Method	Au ₂		Au ₃	
	ζ_1^{1D} ($\times 10^{-3}$)	$\zeta_1^{1D}/\zeta_2^{1D}/\zeta_3^{1D}$ ($\times 10^{-3}$)	$\zeta_{1,2}^{2D}/\zeta_{1,3}^{2D}/\zeta_{2,3}^{2D}$ ($\times 10^{-3}$)	
PBE/VDB	8.9	1.0/3.8/0.5	220/37/85	
BP86/VDB	8.8	1.0/4.0/0.5	220/37/87	
BLYP/VDB	8.6	1.0/3.9/0.4	216/31/71	
LDA/VDB	9.3	1.0/4.2/0.6	231/37/95	

Due to the similar level of theory for these DFT approaches, it is difficult to distinguish which of them is the most suitable to be used as a reference. Thus a comparison to experimental values would be necessary to assess the various DFT approaches. For the case when different levels of theory are involved, as in the comparison of empirical potentials to DFT, the compared values may show larger deviations with respect to the reference, so making easier to realize relative differences between the empirical results.

We have reported a brief version of this comparison elsewhere. [55] Here we recall the main results and extend on their explanation. Figure 2 shows calculated binding energies for the various DFT approaches used, compared to own MP2 results and values reported in other studies. Among the DFT approaches studied, we found PBE/VDB as the most suitable DFT model to reproduce the experimental binding energies of Au₂ (1.15 eV/atom) and Au₃ (1.27 eV/atom), and the experimental bond length of Au₂ dimer (2.47 Å). [56] Experimental binding energies and bond lengths for larger gold clusters have not been reported. For Au₂, bond length is 2.50 Å using PBE/VDB, while Ghiringhelli *et al.* [54] report 2.51 Å using PBE+vdW. Binding energy using PBE/VDB is -1.16 eV/atom, which is similar to the one reported by Ghiringhelli *et al.* using PBE+vdW (-1.18 eV/atom). In a previous study of the Au₇ cluster, [57] we showed that PBE with a pseudo potential basis set such as Goedecker (GTH) or Vanderbilt (VDB) provides a reliable method to describe trends in small gold clusters. For ex-

ample, PBE/VDB predicts the vibrational frequencies of the Au₇ cluster better than other DFT approaches and predicts its global minimum energy structure in agreement with experimental results. [58] Concerning the other DFT approaches investigated, the BP86 functional provides results very close to PBE. On average, the BLYP functional leads to differences in binding energies of about 0.2 eV compared to PBE. For the local density approximation (LDA) functional, a good agreement with the bond length of Au₂ is achieved, but the binding energies of Au₂ and Au₃ are overestimated by ~ 30 % when compared to the experimental values (not shown in Fig. 2).

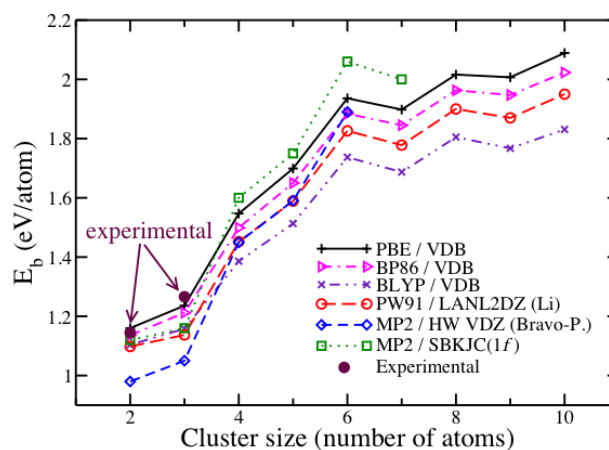


Figure 2: DFT and MP2 calculations, compared to values reported for DFT by Li, [59] and for MP2 by Bravo-Perez, [60] and with experimental values reported by Bishea. [61, 62] All structures are planar. MP2 global minimum energy structure for Au₇ is non-planar but here we show the value corresponding to the planar structure. For Au₃, the structure reported by Bravo-Perez is the equilateral triangle instead of the obtuse triangle.

By comparing our PBE/VDB results with values obtained in other DFT studies, we find that the binding energies are in close agreement with the values reported by Li *et al.* [59] when using the PW91 functional [63] and a LANL2DZ basis set (~ 0.1 eV more on average). Idrobo *et al.*, [64] using the PBE functional with relativistic semicore potentials, report higher binding energies than the ones we obtained (~ 0.15 eV/atom more on average). In comparison with results from Majumder *et al.*, [41] who also used ultrasoft pseudo potentials with a GGA functional, we obtained bond lengths that are shorter by ~ 0.02 Å, and energy values that are slightly larger for Au₂ and Au₃. Binding energies reported by Xiao *et al.*, [65] who use the PW91 functional with the projector augmented wave (PAW) method, are very close to our results (differences by ~ 0.01 eV/atom). On the other hand, studies using PBE with Troullier-Martins norm-conserving pseudo potentials show values different from typical DFT results, *i.e.* Fernandez *et al.* [66] report largely overestimated binding energies, while Rogan *et al.* [30] obtain largely underestimated binding energies.

Concerning other possible high-level theory methods that could be used as a reference for the comparison of empirical potentials, we discuss here briefly results of other studies reported in the literature that use different electronic structure methods, in particular MP2 and CCSD(T). While several studies

of gold clusters have been performed using DFT, [41, 59, 65–73] only a few studies have been performed using the MP2 or CCSD(T) methods, focusing mainly on the Au₂-Au₈ clusters. [12, 32, 42, 46, 60, 74–76] Some studies combine DFT and *ab initio* results, but focus only on a few structures such as Au₂ and Au₃. [77, 78] A few *ab initio* calculations, using single-reference and multireference methods have also been reported. [79–84] It is known that MP2 leads to bond distances that are too short and dissociation energies that are too low for the gold dimer. This is attributed to an overestimation of electron correlation effects. [75, 85] A study of Au₃ to Au₇ clusters by Hermann *et al.* [32] shows that the correlation energy calculated by means of an *n*-body expansion using MP2 does not converge smoothly, thus failing to predict properly the energy and geometry of small metallic clusters. In our previous study, [57] we showed that although MP2 predicts the harmonic frequencies of Au₇ in good agreement with the experimental values, it does not predict well the global minimum energy geometry for this cluster. Moreover, these results of MP2 are presumably a fortuitous effect of the basis set superposition error. [86, 87] Other studies have shown that the CCSD(T) method reproduces the experimental values (bond length and binding energy) of Au₂ better than MP2. [12, 54, 75] Nevertheless, due to the computational cost of applying high-level *ab initio* methods such as MP2 or CCSD(T) that scale faster with cluster size than DFT, and considering that PBE/VDB is suitable for a relatively good prediction of some experimental values of small gold clusters, we chose this DFT approach as the reference method for comparison of empirical potentials. Note that DFT scales with cluster size *N* as $\sim N^3 - N^4$, while MP2 and CCSD(T) scale as $\sim N^5$ and $\sim N^6$, respectively.

4. Assessment of the quality of the empirical potentials

We study five different typical empirical models: The Murrell-Mottram potential [2] with both the parameters used by Wilson and Johnston [19] and the parameters used by Cox, [3] the Sutton-Chen potential, [6] the Gupta potential [4] with the parametrization defined by Cleri and Rosato, [5] the Voter-Chen version of the EAM model, [7–9] and the Glue model as developed by Ercolessi *et al.* [1] The Glue model has been designed to be used in molecular-dynamics simulations of systems in which the coordination number is similar to the one in the bulk regime. It has been applied to study gold surface reconstructions [1] and melting in gold particles with several hundreds of atoms. [29] For very small lead clusters, this potential yields structures different from the ones obtained using the Gupta potential, as reported by Doye. [88, 89] The DBF [10, 11] version of the EAM model is not studied here since it has been shown that this potential largely overestimates the binding energy in small gold clusters. [26, 27] For additional details, such as functional form or specific parameters, we refer the reader to the original studies. Results reported here for the Murrell-Mottram potential correspond to the parameters suggested by Wilson and Johnston. [19] We obtained very similar binding energies with the parameters suggested by Cox, [3] but in that particular case,

planar structures for Au₄, Au₅ and Au₆ were obtained as local minima without using constraints.

In order to make a global comparison of these various potentials, the following should be taken into account: i) The structures predicted by the empirical potentials for gold clusters are planar only for the trivial cases Au₂ and Au₃. However, when using high-level methods, *e.g.* DFT and *ab initio* methods, they are planar up to larger sizes. ii) Comparing only binding energies and bond lengths can lead to misleading results, since each empirical potential has a different functional form and has been fitted in a different way. iii) The choice of a high-level theory as reference model should guarantee a good agreement with experimental values.

For the assessment, we consider three different sets of structures: i) The global minimum energy structures obtained with the empirical potentials, which are non-planar except for the trivial cases Au₂ and Au₃ (see Fig. 3). ii) The global minimum energy structures obtained using PBE/VDB, which are all planar (see Fig. 4). iii) Planar local minimum energy structures predicted by the empirical potentials by using geometrical constraints during the minimization. They have similar but not identical geometries (same or similar symmetry but different bond lengths) when compared to the DFT global minimum energy structures shown in Fig. 4.

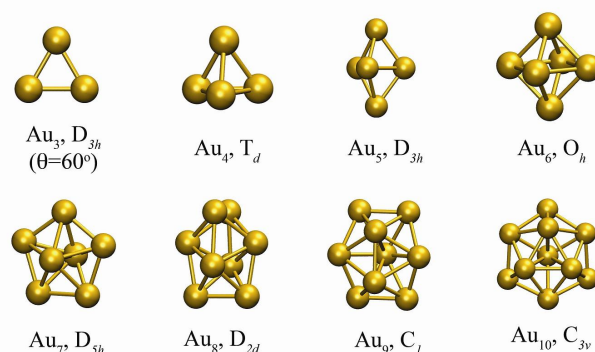


Figure 3: Global minimum energy structures for Au₃-Au₁₀ clusters, along their symmetry point group obtained for the empirical potentials. The Glue potential leads to different minimum energy structures for all clusters. The Murrell-Mottram potential leads to a different minimum energy structure for Au₉ and Au₁₀. Since we compare only the most common minima, those different structures obtained for the Glue and the Murrell-Mottram potential are not shown here.

4.1. Comparison of binding energies and bond lengths

Figure 5 shows the binding energy of the global minimum energy structures obtained without constraints for each potential. The Voter-Chen potential shows intermediate values compared to the other potentials. The Gupta and the Sutton-Chen potentials have similar binding energies to each other but they are both higher than the Voter-Chen potential. The Murrell-Mottram and Glue potentials yield lower binding energies than the Voter-Chen potential. Note that we compare absolute values of the binding energies since we consider these as positive by convention.

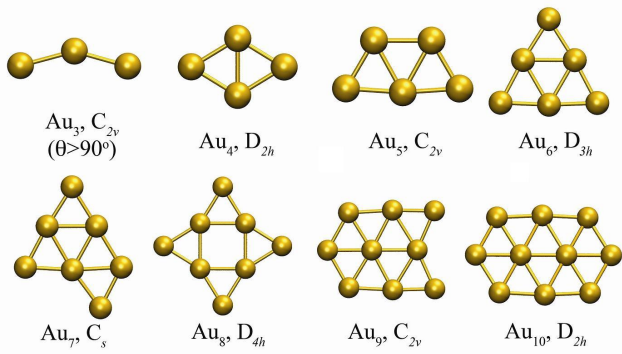


Figure 4: Global minimum energy structures for Au_3 - Au_{10} clusters obtained for PBE/VDB, along their symmetry point group. Structures with equivalent but not identical geometry can be obtained from the empirical potentials by including constraints.

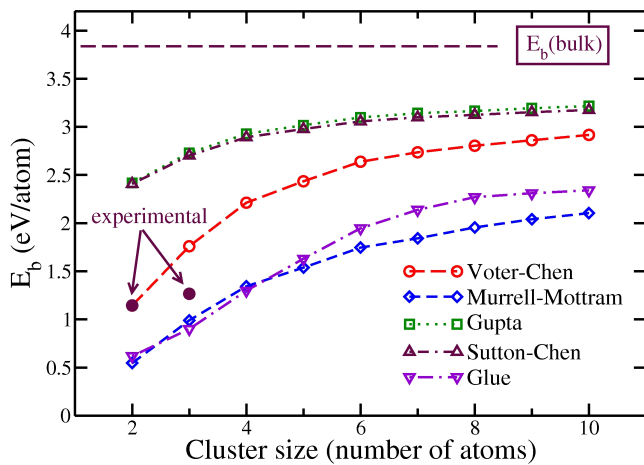


Figure 5: Binding energies calculated for Au_2 - Au_{10} clusters, using different empirical potentials. The values correspond to the global minimum energy structures, which are always non-planar (except for the trivial cases Au_2 and Au_3).

Figure 6(a) shows the binding energies for the planar structures obtained with each empirical potential (using constraints) and with PBE/VDB. Binding energies are best predicted by the Voter-Chen potential. The Voter-Chen parametrization is based on bulk properties but also on the bond length and bond strength of the diatomic molecule, then it is expected to reproduce better the interactions for small molecules but also to have a good behavior towards the bulk regime. Indeed, Alamanova *et al.* [25] and Sebetci *et al.* [24] have shown that the Voter-Chen potential converges to the reported bulk energy (3.82 ± 0.02 eV). [90] The Murrell-Mottram potential shows a relatively good agreement with PBE/VDB, and the Gupta and Sutton-Chen potentials overbind these DFT values by ~ 1 eV/atom. Figure 6(b) shows the binding energy for each potential at the PBE/VDB global minimum energy structures. In all cases, the empirical binding energies are slightly lower than the binding energies obtained at their own empirical planar minima. As a consequence, the Voter-Chen potential becomes the one closest to the PBE/VDB binding energies.

Figure 7(a) shows the average nearest-neighbors bond length

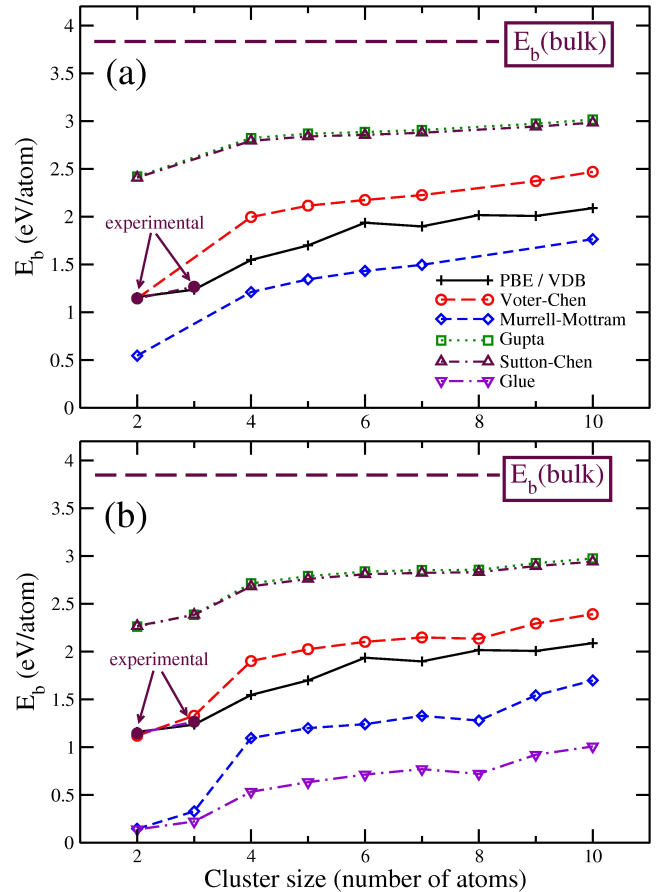


Figure 6: Binding energy for different empirical potentials compared with PBE/VDB results. (a) At the global minimum energy planar structures obtained with each empirical potential (they have similar geometry but are not identical). Glue potential is not included. (b) At the global minimum energy planar structures optimized at DFT level (they are identical).

for the planar minima obtained with PBE/VDB and with the empirical potentials. Structures corresponding to each method for each cluster size have similar geometry but are not identical. The Voter-Chen, Sutton-Chen and Gupta potentials lead to bond lengths shorter than PBE/VDB. For the Sutton-Chen and Gupta potentials these bonds are larger than those predicted by Voter-Chen, except for Au_2 . The Murrell-Mottram potential leads to structures with larger bond lengths than PBE/VDB.

Considering the reported experimental value of 4.0786 ± 0.0002 Å for the lattice constant of the fcc gold structure, [90] the experimental nearest-neighbors bond length for the bulk is estimated as 2.8840 ± 0.0002 Å. It is desirable that the potentials converge to that value in the bulk regime, but with values only up to $n = 10$ is not possible to predict that convergence. Nevertheless, it is observed that the Gupta, Sutton-Chen and Voter-Chen potentials have a monotonically increasing nearest-neighbors bond length while for the Murrell-Mottram potential this magnitude is almost uniform at different cluster sizes.

Following the procedure described by Grigoryan *et al.*, [28] a similarity factor S was obtained for each method and for each cluster size, derived from the root mean square (rms) value of the differences of all interatomic distances. The similarity

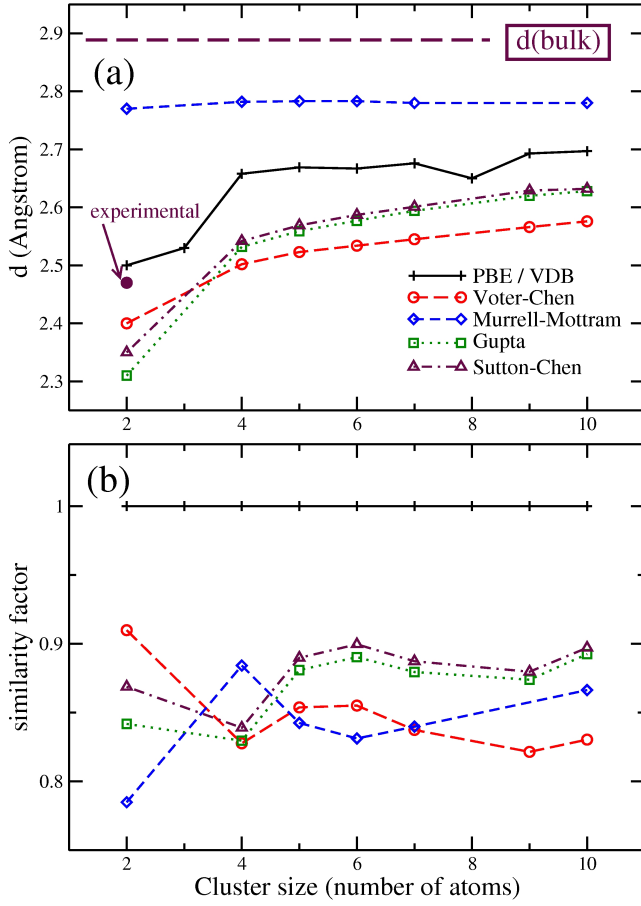


Figure 7: Comparison of bond lengths obtained using empirical potentials and PBE/VDB. (a) Average bond length between nearest-neighbors for planar structures equivalent to the DFT minima. (b) Similarity factor for the different methods considering all interatomic distances. PBE/VDB is the reference ($s = 1$). The closer to $s = 1$ the more similar to the reference.

factor, S , will approach one as the value for q goes towards zero, that indicates a larger similarity between the geometry of two structures compared.

$$S = \frac{1}{1+q}, \quad (8)$$

$$q = \left[\frac{2}{N(N-1)} \sum_{i=1}^{N(N-1)/2} (d_i - d_i^{ref})^2 \right]^{1/2}. \quad (9)$$

The distances d_i and d_i^{ref} (in Å) correspond to the interatomic distances of the structure to be compared and those of the structure which acts as a reference, respectively. The same definition for q has been recently used by Rogan *et al.* [91] to compare Gupta, Sutton-Chen and Lennard-Jones potentials for small nickel and copper clusters.

Figure 7(b) shows the values of the similarity factor for the empirical potentials compared to the one for PBE/VDB ($s = 1$). It shows that the structures predicted by the various empirical po-

tentials show similarity factors between 0.8 and 0.9, and that the similarity is better for Gupta and Sutton-Chen potentials for Au_5 and larger clusters. Conclusions obtained from the similarity factor criterion are in agreement to those obtained by looking at the average nearest-neighbors bond length. Nevertheless, since the outcome is based on a rms value, it does not show the direction of the distance changes for each structure in comparison with the reference. The average bond length or the similarity factor are not sufficient criteria to evaluate the quality of empirical potentials, although they provide valuable information. For example, the Voter-Chen potential, which yields binding energies closer to PBE/VDB, underestimates the bond lengths. The Sutton-Chen and Gupta potentials, which largely overestimate the binding energy, underestimate the bond lengths less than the Voter-Chen potential does, in comparison with PBE/VDB. The analysis of Hermann *et al.* [32] is also not well suited to assess the quality of the empirical potentials. They observe that the Glue potential well resembles the many-body expansion of the interaction potential for the planar Au_7 cluster when compared with MP2. Nevertheless, we observe that this potential leads to structures very different from the ones obtained using other empirical potentials, and underestimates both the bond lengths and binding energies.

4.2. Comparison of the 1D potential energy curves

Table 2 shows all calculated indices compared to PBE/VDB. For Au_2 and each empirical potential, the 1D index is too large in comparison to PBE/VDB, leading to a poor description of the 1D potential energies. For the Glue and Voter-Chen potential, this value is closer but still more than two times higher than PBE/VDB. For Au_3 , only the Voter-Chen and Gupta potentials achieve a value close to PBE/VDB for ζ_1^{1D} , which describes the antisymmetric stretch mode of the molecule. For the same cluster all potentials lead to absolute values of ζ_2^{1D} and ζ_3^{1D} that differ a lot from PBE/VDB. These two indices describe the breathing and the bending mode of the molecule, respectively. Only the Glue potential achieves a value close to PBE/VDB for ζ_3^{1D} . By normalizing the 1D indices to the largest index of each method, ζ_2^{1D} , we observe that the Voter-Chen potential is the one which closely resembles ζ_3^{1D} . All of them fail to reproduce the values of ζ_1^{1D} properly.

Table 2: Comparison of various empirical potentials to PBE/VDB. 1D indices for Au_2 and Au_3 , and 2D indices for Au_3 are referred to PBE/VDB and scaled by 10^3 .

Method	Au ₂	Au ₃	
	ζ_1^{1D} ($\times 10^{-3}$)	$\zeta_1^{1D}/\zeta_2^{1D}/\zeta_3^{1D}$ ($\times 10^{-3}$)	$\zeta_2^{2D}/\zeta_{1,3}^{2D}/\zeta_{2,3}^{2D}$ ($\times 10^{-3}$)
PBE/VDB	8.9	1.0/3.8/0.5	220/37/85
Voter-Chen	44.5	0.6/54.2/7.7	165/27/77
Murrell-Mottram	464.5	5.3/479.8/9.8	1103/193/595
Gupta	149.4	1.3/131.0/5.7	218/34/109
Sutton-Chen	156.8	3.1/136.7/7.0	382/56/132
Glue	19.5	0.1/13.2/0.4	5/4/14

Figure 8(a) shows the six 1D indices obtained for Au₄. For a suitable comparison they are normalized to the value of the index ζ_3^{1D} for each set of values. Only for ζ_2^{1D} , ζ_5^{1D} and ζ_6^{1D} do all empirical potentials reproduce the relative magnitude of the index with respect to the reference index ζ_3^{1D} . The Glue potential shows a lesser agreement in comparison with the other ones. None of the potentials reproduce ζ_1^{1D} and ζ_4^{1D} , which correspond to the breathing and the bending mode of the molecule, respectively. An exception is ζ_4^{1D} , which is roughly reproduced by Murrell-Mottram. Figure 8(b) shows the nine 1D indices for Au₅. For a suitable comparison they are normalized to the value of the index ζ_1^{1D} for each set of values. None of the potentials reproduce the relative magnitude of ζ_2^{1D} (breathing mode) and ζ_3^{1D} with respect to the reference index ζ_1^{1D} . Index ζ_4^{1D} is well predicted by all potentials, ζ_5^{1D} and ζ_6^{1D} are partially reproduced only by the Voter-Chen potential, and the remaining indices show a reasonable agreement with PBE/VDB for all potentials used.

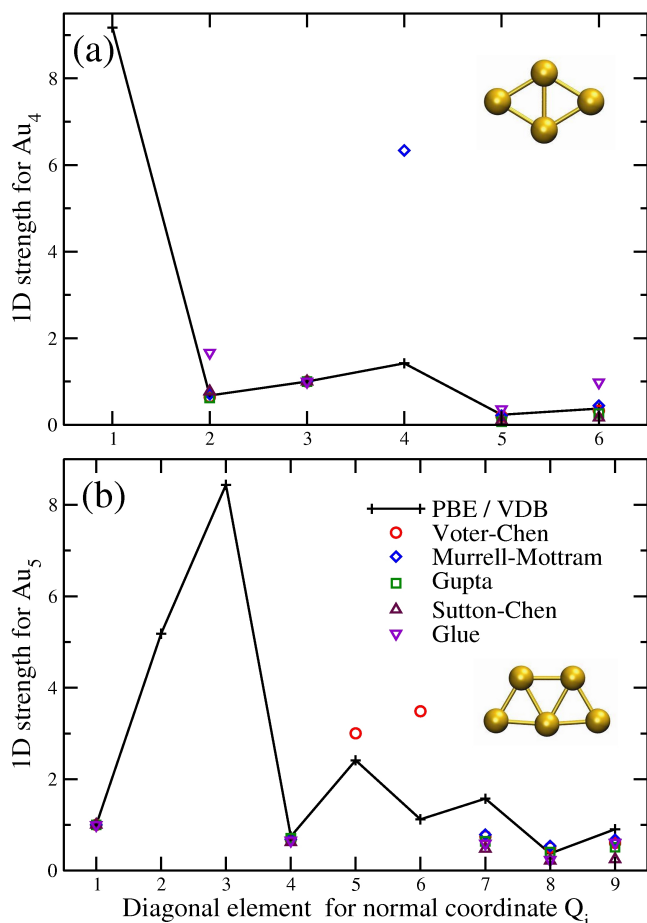


Figure 8: Values of the 1D indices, as calculated with PBE/VDB and with empirical potentials. (a) Au₄: empirical potentials do not reproduce the DFT values for the indices 1 and 4; therefore, badly predicted values were omitted and the remaining ones were normalized to the value of the index 3 for each set of values. (b) Au₅: empirical potentials do not reproduce the DFT values for the indices 2, 3, 5 and 6 (Voter-Chen does not reproduce 2 and 3 but it does with 5 and 6); therefore, badly predicted values were omitted and the remaining ones normalized to the value of the index 1 for each set of values.

For Au₄ and Au₅, all potentials fail to completely reproduce the main features of the 1D potential energy curves obtained using PBE/VDB, although the Voter-Chen potential makes a better description than the other potentials.

4.3. Comparison of the 2D potential energy surfaces

We investigate how all potentials studied reproduce the PBE/VDB reference 2D PES. For Au₃, the best agreement with the PBE/VDB values is obtained by the Voter-Chen and the Gupta potential (see Table 2). All potentials except the Glue model reproduce the same order of the PBE/VDB 2D indices. For a suitable comparison for Au₄ and Au₅, we normalize each 2D index to the largest value for each method and then organize all values according to the order obtained using PBE/VDB.

Figure 9(a) shows the 2D indices obtained for Au₄ (15 couplings). In this case, the Voter-Chen and Murrell-Mottram potentials reproduce better the order and magnitude of the 2D indices showing the lowest rms values. Figure 9(b) shows the 2D indices for Au₅ (36 couplings). Again, the Voter-Chen potential shows the best agreement with PBE/VDB. The few indices that vary significantly from those obtained with PBE/VDB do not affect the order at the pair-couplings with the highest values of the index. The Murrell-Mottram potential shows very large values for some indices that correspond to small values in the reference 2D PES, thus largely affecting the order of the indices. For both Au₄ and Au₅, the Sutton-Chen and Gupta potentials lead to large deviations from the 2D indices obtained with PBE/VDB. As a consequence, the order of the indices is largely affected. The Glue potential leads to very large deviations of the index values, therefore it does not reproduce the order of these indices properly (indices for Glue potential are not shown in Fig. 9).

5. Conclusions and remarks

Comparing only average bond lengths or binding energies is not sufficient to decide if a certain empirical potential is suitable to reproduce high-level theory results. Instead, investigating how each potential reproduces the potential energy surface obtained with high level theory, gives a deeper insight into its features. Therefore, we proposed a local comparison of 1D and 2D potential energies, expressing the position of the atoms in terms of normal coordinates. Of the various DFT approaches studied, the PBE functional with a plane-wave basis set and a Vanderbilt pseudo potential (PBE/VDB) yields the best agreement with experimental binding energies. Consequently, we chose this approach as the reference method for the comparison of the empirical potentials.

All empirical potentials studied fail to reproduce completely the 1D potential energy curves obtained with PBE/VDB. Nevertheless, the Voter-Chen potential and the Murrell-Mottram potential, to a lesser degree, behave better than the others and reproduce partially the PBE/VDB 1D curves. All of them fail to reproduce the index associated with the breathing mode of the molecule and to a lesser degree the index associated to the bending mode. The Voter-Chen potential is the most suitable for reproducing the ordering of the normalized 2D indices obtained

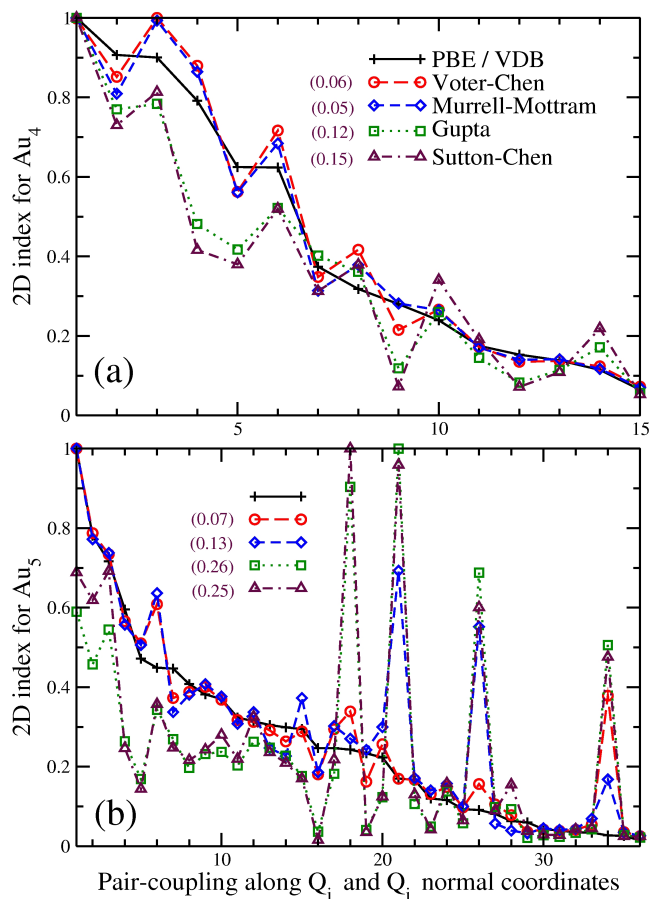


Figure 9: 2D indices for (a) Au_4 and (b) Au_5 , as calculated with PBE/VDB and various empirical potentials. They are shown following the order of the DFT values. Each set of values is normalized to its own highest value. Results from the Glue potential are omitted because of their larger deviations from DFT. Values in parenthesis denote root mean square deviations (RMSD) from the PBE/VDB reference values.

using PBE/VDB even if the differences on absolute values are large. The performance of the Murrell-Mottram potential is still adequate but fails to reproduce properly some indices at the largest values of the pair couplings. For the Gupta, Sutton-Chen and Glue potentials, the agreement to the order of 2D indices is not satisfactory.

The Voter-Chen potential reproduces the DFT binding energies better, although it underestimates the bond lengths more than the Gupta and Sutton-Chen potentials. The Glue potential does not reproduce the same structures as the other potentials, and largely underestimates bond lengths and binding energies. Since this potential has been developed for bulk systems, the result is not surprising. The Murrell-Mottram potential predicts structures with regular bond lengths. With the parameters suggested by Cox *et al.*, it is the only potential predicting planar structures without constraints.

We have introduced an alternative methodology in order to reveal the main differences between empirical potentials. These empirical potentials are often cataloged as unreliable for describing structural and energetic properties accurately compared to high-level theory. For the case of very small gold clusters, we

have observed that they can partially reproduce some of these properties, *i.e.* some of them can make predictions of the bond lengths or the energies better than other potentials. However, a simultaneous prediction of structural and energetic values is not observed. Although the use of geometrical constraints is necessary in order to reproduce the planar geometries predicted by high-level theory, the methodology presented here provides a valuable criterion to compare these and eventually other empirical potentials.

Acknowledgments

This work was supported by a grant ("SFB-569/TP-N1") from the German Science Foundation (DFG) through the Special Research Unit "Hierarchical Structure Formation and Function of Organic-Inorganic Nanosystems". We thank A. F. Voter (Los Alamos National Laboratory) for providing information about his method, and L. Leick for proofreading the manuscript.

References

- [1] F. Ercolessi, M. Parrinello, E. Tosatti, Simulation of gold in the glue model, *Phil. Mag. A* 58 (1) (1988) 213–226.
- [2] J. N. Murrell, R. Mottram, Potential energy function for atomic solids, *Mol. Phys.* 69 (3) (1990) 571–585.
- [3] H. Cox, X. Liu, J. N. Murrell, Modelling Cu, Ag and Au surfaces using empirical potentials, *Mol. Phys.* 93 (6) (1998) 921–924.
- [4] R. J. Gupta, Lattice relaxation at a metal surface, *Phys. Rev. B* 23 (12) (1981) 6265–6270.
- [5] F. Cleri, V. Rosato, Tight-binding potentials for transition metal and alloys, *Phys. Rev. B* 48 (1) (1993) 22–33.
- [6] A. P. Sutton, J. Chen, Long-range Finnis-Sinclair potentials, *Phil. Mag. Letters* 1990 (3) (1990) 139–146.
- [7] A. F. Voter, Embedded atom method potentials for seven fcc metals: Ni, Pd, Pt, Cu, Ag, Au, and Al, Tech. Rep. LA-UR 93-3901, Los Alamos, unclassified (1993).
- [8] A. F. Voter, S. P. Chen, Accurate interatomic potentials for Ni, Al and Ni_3Al , *Mat. Res. Soc. Symp. Proc.* 82 (1987) 175–180.
- [9] A. F. Voter, *Intermetallic Compounds*, Vol. 1, Wiley, 1994, Ch. 4, The embedded-atom method.
- [10] M. S. Daw, M. I. Baskes, Embedded-atom method: Derivation and application to impurities, surfaces and other defects in metals, *Phys. Rev. B* 29 (12) (1984) 6443–6453.
- [11] S. M. Foiles, M. I. Baskes, M. S. Daw, Embedded-atom method functions for the fcc metals Cu, Ag, Au, Ni, Pd, Pt and their alloys, *Phys. Rev. B* 33 (12) (1986) 7983–7991.
- [12] R. Wesendrup, T. Hunt, P. Schwerdtfeger, Relativistic coupled cluster calculations for neutral and singly charged Au_3 clusters, *J. Chem. Phys.* 112 (2000) 9356–9362.
- [13] P. Pykkö, Relativistic effects in structural chemistry, *Chem. Rev.* 88 (3) (1988) 563–594.
- [14] P. Pykkö, Theoretical chemistry of gold, *Angew. Chem. Int. Ed.* 43 (34) (2004) 4412–4456.
- [15] P. Pykkö, Theoretical chemistry of gold II, *Inorg. Chim. Acta* 358 (14) (2005) 4113–4130.
- [16] P. Schwerdtfeger, Gold goes nano: From small clusters to low-dimensional assemblies, *Angew. Chem. Int. Ed.* 42 (17) (2003) 1892–1895.
- [17] S. A. Serapian, M. J. Bearpark, F. Bresme, The shape of Au_8 : gold leaf or gold nugget?, *Nanoscale* 5 (2013) 6445–6457.
- [18] S. Heiles, A. J. Logsdail, R. Schafer, R. L. Johnston, Dopant-induced 2D-3D transition in small Au-containing clusters: DFT-global optimisation of 8-atom Au-Ag nanoalloys, *Nanoscale* 4 (2012) 1109–1115.
- [19] N. T. Wilson, R. L. Johnston, Modelling gold clusters with an empirical many-body potential, *Eur. Phys. J. D.* 12 (1) (2000) 161–169.
- [20] K. Michaelian, N. Rendon, I. L. Garzon, Structure and energetics of Ni, Ag and Au nanoclusters, *Phys. Rev. B* 60 (3) (1999) 2000–2010.

- [21] I. L. Garzon, K. Michaelian, M. R. Beltran, A. Posada-Amarillas, P. Ordejon, E. Artacho, D. Sanchez-Portal, J. M. Soler, Lowest energy structures of gold nanoclusters, *Phys. Rev. Lett.* 81 (8) (1998) 1600–1603.
- [22] I. L. Garzon, K. Michaelian, M. R. Beltran, A. Posada-Amarillas, P. Ordejon, E. Artacho, D. Sanchez-Portal, J. M. Soler, Structure and thermal stability of gold nanoclusters: the Au₃₈ case, *Eur. Phys. J. D* 9 (1) (1999) 211–215.
- [23] I. L. Garzon, A. Posada-Amarillas, Structural and vibrational analysis of amorphous Au₅₅ clusters, *Phys. Rev. B* 54 (16) (1996) 11796–11802.
- [24] A. Sebetci, Z. B. Güvenç, Global minima of Al_N, Au_N and Pt_N, ($n \leq 80$), clusters described by the voter-chen version of embedded-atom potentials, *Modelling Simul. Mater. Sci. Eng.* 13 (5) (2005) 683–698.
- [25] D. Alamanova, V. G. Grigoryan, M. Springborg, Theoretical study of structure and energetics of gold clusters with the eam method, *Z. Phys. Chemie* 220 (7) (2006) 811–829.
- [26] C. Rey, L. J. Gallego, J. Garcia-Rodeja, J. A. Alonso, M. P. Iniguez, Molecular-dynamics study of the binding energy and melting of transition-metals clusters, *Phys. Rev. B* 48 (11) (1993) 8253–8262.
- [27] J. Garcia-Rodeja, C. Rey, L. J. Gallego, Molecular-dynamics study of the structures, binding energies, and melting of clusters of fcc transition and noble metals using the Voter and Chen version of the embedded-atom model, *Phys. Rev. B* 49 (12) (1994) 8495–8498.
- [28] V. G. Grigoryan, D. Alamanova, M. Springborg, Structure and energetics of nickel, copper and gold clusters, *Eur. Phys. J. D.* 34 (1-3) (2005) 187–190.
- [29] F. Ercolessi, W. Andreoni, E. Tosatti, Melting of small gold particles: Mechanism and size effects, *Phys. Rev. Lett.* 66 (7) (1991) 911–914.
- [30] J. Rogan, R. Ramirez, A. H. Romero, M. Kiwi, Rearrangement collisions between gold clusters, *Eur. Phys. J. D* 28 (2) (2004) 219–228.
- [31] J. P. Perdew, K. Burke, M. Ernzerhof, Generalized gradient approximation made simple, *Phys. Rev. Lett.* 77 (18) (1996) 3865–3868.
- [32] A. Hermann, R. P. Krawczyk, M. Lein, P. Schwerdtfeger, I. P. Hamilton, J. J. P. Stewart, Convergence of the many-body expansion of interaction potentials: From van der Waals to covalent and metallic systems, *Phys. Rev. A* 76 (2007) 013202–10.
- [33] N. J. Wright, R. B. Gerber, Direct calculation of anharmonic vibrational states of polyatomic molecules using potential energy surfaces calculated from density functional theory, *J. Chem. Phys.* 112 (6) (2000) 2598–2604.
- [34] D. M. Benoit, Fast vibrational self-consistent field calculations through a reduced mode-mode coupling, *J. Chem. Phys.* 120 (2) (2004) 562–573.
- [35] IBM Corp. and MPI Stuttgart, CPMD Code, version 3.11.1, Car-Parrinello Molecular Dynamics (March 2005).
- [36] A. D. Becke, Density-functional exchange-energy approximation with correct asymptotic behavior, *Phys. Rev. A* 38 (6) (1988) 3098–3100.
- [37] J. P. Perdew, Density-functional approximation for the correlation energy of the inhomogeneous electron gas, *Phys. Rev. B* 33 (12) (1986) 8822–8824.
- [38] C. Lee, W. Yang, R. G. Parr, Development of the Colle-Salvetti correlation-energy formula into a functional of the electron density, *Phys. Rev. B* 37 (2) (1988) 785–789.
- [39] J. P. Perdew, A. Zunger, Self-interaction correction to density-functional approximations for many-electron systems, *Phys. Rev. B* 23 (10) (1981) 5048–5079.
- [40] D. Vanderbilt, Soft self-consistent pseudopotentials in a generalized eigenvalue formalism, *Phys. Rev. B* 41 (11) (1990) 7892–7895.
- [41] C. Majumder, S. K. Kulshreshtha, Structural and electronic properties of Au_n ($n=2-10$) clusters and their interactions with single S atoms: *Ab initio* molecular dynamics simulations, *Phys. Rev. B* 73 (15) (2006) 155427–10.
- [42] R. M. Olson, S. Varganov, M. S. Gordon, H. Metiu, S. Chretien, P. Piecuch, K. Kowalski, S. A. Kucharski, M. Musial, Where does the planar-to-nonplanar turnover occur in small gold clusters?, *J. Am. Chem. Soc.* 127 (3) (2005) 1049–1052.
- [43] S. R. Billeter, A. Curioni, W. Andreoni, Efficient linear scaling geometry optimization and transition-state search for direct wavefunction optimization schemes in density functional theory using a plane-wave basis, *Comp. Mater. Sci.* 27 (4) (2003) 437–445.
- [44] M. W. Schmidt, K. K. Baldridge, J. A. Boatz, S. T. Elbert, M. S. Gordon, J. H. Jensen, S. Koseki, N. Matsunaga, K. A. Nguyen, S. Su, T. L. Windus, M. Dupuis, J. A. M. Jr., General atomic and molecular electronic structure system, *J. Comput. Chem.* 14 (11) (1993) 1347–1363, GAMESS code, version 11 (2008).
- [45] W. J. Stevens, M. Krauss, H. Basch, P. G. Jasien, Relativistic compact effective potentials and efficient, shared-exponent basis sets for the third-, fourth-, and fifth-row atoms, *Can. J. Chem.* 70 (2) (1992) 612–630.
- [46] R. M. Olson, M. S. Gordon, Isomers of Au₈, *J. Chem. Phys.* 126 (2007) 214310–6.
- [47] J. C. Lagarias, J. A. Reeds, M. H. Wright, P. E. Wright, Convergence properties of the Nelder-Mead simplex method in low dimensions, *SIAM J. Optim.* 9 (1) (1998) 112–147.
- [48] J. A. Nelder, R. Mead, A simplex method for function minimization, *Comput. Journal* 7 (4) (1965) 308–313.
- [49] W. Press, S. Teukolsky, W. Vetterling, B. Flannery, Numerical Recipes in Fortran, 2nd Edition, Cambridge University Press, 1996.
- [50] L. A. Mancera, EPOCUS Code, version 1.0 (2012).
- [51] D. M. Benoit, I. Respondek, B. Madebene, Y. Scribano, D. M. Lauvergnat, PVSCF code, latest version (2009).
- [52] H. Akima, Algorithm 760: Rectangular-grid-data surface fitting that has the accuracy of a bicubic polynomial, *ACM Transactions on Mathematical Software (TOMS)* 22 (3) (1996) 357–361.
- [53] W. Humphrey, A. Dalke, K. Schulten, Vmd - visual molecular dynamics, *J. Mol. Graphics* 14 (1) (1996) 33–38.
- [54] L. M. Ghiringhelli, P. Gruene, J. T. Lyon, D. M. Rayner, G. Meijer, A. Fielicke, M. Scheffler, Not so loosely bound rare gas atoms: finite-temperature vibrational fingerprints of neutral gold-cluster complexes, *New J. Phys.* 15 (8) (2013) 083003–22.
- [55] D. M. Benoit, B. Madebene, I. Ulusoy, L. A. Mancera, Y. Scribano, S. Chulkov, Towards a scalable and accurate quantum approach for describing vibrations of molecule-metal interfaces, *Beilstein J. Nanotechnol.* 2 (2011) 427–447.
- [56] M. Morse, Clusters of transition-metal atoms, *Chem. Rev.* 86 (6) (1986) 1049–1109.
- [57] L. A. Mancera, D. M. Benoit, Towards an understanding of the vibrational spectrum of the neutral au₇ cluster, *Phys. Chem. Chem. Phys.* 15 (2013) 1929–1943.
- [58] P. Gruene, D. M. Rayner, B. Redlich, A. F. G. van der Meer, J. T. Lyon, G. Meijer, A. Fielicke, Structures of neutral Au₇, Au₁₉ and Au₂₀ clusters in the gas phase, *Science* 321 (5889) (2008) 674–676.
- [59] X.-B. Li, H.-Y. Wang, X.-D. Yang, Z.-H. Zhu, Y.-J. Tang, Size dependence of the structures and energetic and electronic properties of gold clusters, *J. Chem. Phys.* 126 (2007) 084505–8.
- [60] G. Bravo-Perez, I. L. Garzon, O. Novaro, *Ab initio* study of small gold clusters, *J. Mol. Struct. Theochem* 493 (1-3) (1999) 225–231.
- [61] G. Bishea, M. Morse, Spectroscopic studies of jet-cooled AgAu and Au₂, *J. Chem. Phys.* 95 (8) (1991) 5646–5659.
- [62] G. A. Bishea, M. D. Morse, Resonant two-photon ionization spectroscopy of jet-cooled Au₃, *J. Chem. Phys.* 95 (12) (1991) 8779–8792.
- [63] J. P. Perdew, J. A. Chevary, S. H. Vosko, K. A. Jackson, M. R. Pederson, D. J. Singh, C. Fiolhais, Atoms, molecules, solids, and surfaces: Applications of the generalized gradient approximation for exchange and correlation, *Phys. Rev. B* 46 (11) (1992) 6671–6687.
- [64] J. C. Idrobo, W. Walkosz, S. F. Yip, S. Ögüt, J. Wang, J. Jellinek, Static polarizabilities and optical absorption spectra of gold clusters (Au_n, $n=2-14$ and 20) from first principles, *Phys. Rev. B* 76 (20) (2007) 205422–12.
- [65] L. Xiao, B. Tollberg, X. Hu, L. Wang, Structural study of gold clusters, *J. Chem. Phys.* 124 (2006) 114309–10.
- [66] E. M. Fernandez, J. M. Soler, I. L. Garzon, L. C. Balbas, Trends in the structure and bonding of noble metal clusters, *Phys. Rev. B* 70 (16) (2004) 165403–14.
- [67] J. Wang, G. Wang, J. Zhao, Density functional study of Au_n ($n = 2 - 20$) clusters: lowest-energy structures and electronic properties, *Phys. Rev. B* 66 (2002) 035418–6.
- [68] A. V. Walker, Structure and energetics of small gold nanoclusters and their positive ions, *J. Chem. Phys.* 122 (9) (2005) 094310–12.
- [69] V. Bonacic-Koutecky, J. Burda, R. Mitric, M. Ge, G. Zampella, P. Fantucci, Density functional study of structural and electronic properties of bimetallic silver-gold clusters: comparison with pure gold and silver clusters, *J. Chem. Phys.* 117 (7) (2002) 3120–3131.
- [70] H. Häkkinen, U. Landman, Gold clusters (Au_N, $2 \leq N \leq 10$) and their anions, *Phys. Rev. B* 62 (4) (2000) R2287–R2290.
- [71] H. Grönbeck, W. Andreoni, Gold and platinum microclusters and their anions: comparison of structural and electronic properties, *Chem. Phys.* 262 (1) (2000) 1–14.

- [72] H. Grönbeck, P. Broqvist, Comparison of the bonding in Au₈ and Cu₈: a density functional theory study, *Phys. Rev. B* 71 (7) (2005) 073408–4.
- [73] F. Remacle, E. S. Kryachko, Structure and energetics of two- and three-dimensional neutral, cationic and anionic gold clusters Au_{5 ≤ n ≤ 9}^Z (Z = 0, ±1), *J. Chem. Phys.* 122 (4) (2005) 044304–14.
- [74] G. Bravo-Perez, I. L. Garzon, O. Novaro, Non-additive effects in small gold clusters, *Chem. Phys. Lett.* 313 (3-4) (1999) 655–664.
- [75] B. A. Hess, U. Kaldor, Relativistic all-electron coupled-cluster calculations on Au₂ in the framework of the Douglas-Kroll transformation, *J. Chem. Phys.* 112 (4) (2000) 1809–1813.
- [76] Y.-K. Han, Structure of Au₈: Planar or nonplanar?, *J. Chem. Phys.* 124 (2006) 024316–3.
- [77] Y. Shen, J. J. BelBruno, Density functional theory study of the Jahn-Teller effect and spin-orbit coupling for copper and gold trimers, *J. Phys. Chem. A* 109 (3) (2005) 512–519.
- [78] A. A. Rusakov, E. Rykova, G. E. Scuseria, A. Zaitsevskii, Importance of spin-orbit effects on the isomerism profile of Au₃: an *ab initio* study, *J. Chem. Phys.* 127 (2007) 164322–5.
- [79] C. W. Bauschlicher, S. R. Langhoff, H. Patridge, Theoretical study of the structures and electron affinities of the dimers and trimers of the group IB metals (Cu, Ag, and Au), *J. Chem. Phys.* 91 (4) (1989) 2412–2419.
- [80] C. W. Bauschlicher, S. R. Langhoff, H. Patridge, Theoretical study of the homonuclear tetramers and pentamers of the group IB metals (Cu, Ag, and Au), *J. Chem. Phys.* 93 (11) (1990) 8133–8137.
- [81] K. Das, K. Balasubramanian, Spectroscopic properties of low-lying electronic states of Au₂, *J. of Mol. Spectrosc.* 140 (2) (1990) 280–294.
- [82] K. Balasubramanian, K. Das, Excited electronic states of Au₃, *Chem. Phys. Lett.* 186 (6) (1991) 577–582.
- [83] K. Balasubramanian, P. Y. Feng, M. Z. Liao, Geometries and energy separations of 14 electronic states of Au₄, *J. Chem. Phys.* 91 (6) (1989) 3561–3570.
- [84] D. Liao, K. Balasubramanian, Electronic structure of Cu₆, Ag₆, Au₆ and their positive ions, *J. Chem. Phys.* 97 (4) (1992) 2548–2552.
- [85] P. Schwerdtfeger, M. Lein, *Gold Chemistry. Applications and future directions in the life sciences*, Wiley, 2009, Ch. 4, edited by F. Mohr.
- [86] S. F. Boys, F. Bernardi, The calculation of small molecular interactions by the differences of separate total energies. some procedures with reduced errors, *Mol. Phys.* 19 (4) (1970) 553–566.
- [87] P. Salvador, B. Paizs, M. Duran, S. Suhai, On the effect of the BSSE on intermolecular potential energy surfaces. comparison of *a priori* and *a posteriori* BSSE correction schemes, *J. Comput. Chem.* 22 (7) (2001) 765–768.
- [88] J. P. K. Doye, S. C. Hendy, On the structure of small lead clusters, *Eur. Phys. J. D.* 22 (1) (2003) 99–107.
- [89] J. P. K. Doye, Lead clusters: Different potentials, different structures, *Comput. Mater. Sci.* 35 (3) (2006) 227–231.
- [90] D. R. Lide (Ed.), *CRC Handbook of Chemistry and Physics*, 72nd Edition, CRC Press, 1991-1992.
- [91] J. Rogan, M. Ramirez, A. Varas, M. Kiwi, How relevant is the choice of classical potentials in finding minimal energy cluster conformations?, *Comput. Theor. Chem.* 1021 (2013) 155 – 163.